

Assessment of COVID-19 hospitalization forecasts from a simplified SIR model*

P.-A. Absil[§] Ousmane Diao[§] Mouhamadou Diallo[¶]

May 27, 2022

Abstract

We propose the SH model, a simplified version of the well-known SIR compartmental model of infectious diseases. With optimized parameters and initial conditions, this time-invariant two-parameter two-dimensional model is able to fit COVID-19 hospitalization data over several months with high accuracy (mean absolute percentage error below 15%). Moreover, we observed that, when the model is trained on a suitable two-week period around the hospitalization peak for Belgium, it forecasts the subsequent three-month decrease with mean absolute percentage error below 10%. However, when it is trained in the increase phase, it is less successful at forecasting the subsequent evolution.

Key words: COVID-19 prediction; COVID-19 forecast; SARS-CoV-2; coronavirus; SIR model; SH model; hidden variable; hospitalization prediction

1 Introduction

The SIR model [KMW27] is a simple compartmental model that is widely used to model infectious diseases [Het00]. Letting $S(t)$, $I(t)$, and $R(t)$ denote the number of susceptible, infectious and removed (or recovered) individuals at time t , and letting $\dot{S}(t)$, $\dot{I}(t)$, and $\dot{R}(t)$ denote their time derivatives, the SIR model consists in the following three-dimensional continuous-time autonomous dynamical system

$$\dot{S}(t) = -\frac{\beta}{N}S(t)I(t) \tag{1a}$$

$$\dot{I}(t) = \frac{\beta}{N}S(t)I(t) - \gamma I(t) \tag{1b}$$

$$\dot{R}(t) = \gamma I(t), \tag{1c}$$

where $N = S(t) + I(t) + R(t)$ is the constant total population and β and γ are parameters. The SIR model, and several (sometimes deep) variations thereof, have been applied in several works to model the COVID-19 dynamics (see, e.g., [LGWR20, Atk20, Koz20, Nes20, CNP20, FP20, CFP20]) with known limitations (see [RVHL20, BFG⁺20, WF20]). Sometimes, an SIR-like model is used to make long-term predictions (see [BD20]). However, at the time of writing this paper, it appears that studies are still rare (see, e.g., [SM20]) where the SIR model parameters and initial conditions are learned on a “train” part of the available data in order to predict a “test” part of the data, making it possible to assess the prediction accuracy of the model.

In this paper, we adapt the SIR model to the situation where (i) S , I and R are hidden variables but $I(t)$ is observed through a “proxy” $H(t) = \alpha I(t)$, where α is unknown but constant, and (ii)

*The second author is supported by a fellowship awarded by UCLouvain’s Conseil de l’action internationale.

[§]ICTEAM Institute, UCLouvain, B-1348 Louvain-la-Neuve, Belgium (<http://sites.uclouvain.be/absil/>).

[¶]Molecular Biology Unit/Bacteriology-Virology Lab, CNHU A. Le Dantec / Université Cheikh Anta Diop, Dakar, Sénégal

not only β and γ but also the total population N are unknown and have thus to be estimated. In the context of the COVID-19 application, H will stand for the total number of lab-confirmed hospitalized patients. The proposed adapted SIR model, which we term *SH model*, is given in (8). It has two state variables (\bar{S} —a scaled version S —and H) and two parameters ($\bar{\beta}$ —which lumps together the parameters β , N , and α —and γ).

We leverage the proposed SH model as follows in order to make hospitalization predictions. Given observed values $(H_o(t))_{t=t_i, \dots, t_e}$, we estimate the parameters $\bar{\beta}$, γ , and the initial conditions $\bar{S}(t_i)$ and $H(t_i)$ of the SH model. Then we simulate the SH model in order to predict $(H(t))_{t=t_e+1, \dots, t_f}$ for a specified final prediction time t_f . This approach thus combines the areas of parameter estimation (for obvious reasons), data assimilation (for the generation of the initial conditions) and machine learning (for the train-test approach).

2 Data

In Section 6, we will use a COVID-19 dataset for Belgium¹ that provides us with the following data for $t = t_s, \dots, t_e$, where t_s is 2020-03-15 and t_e is 2020-07-15:

- $H_o(t)$: number of COVID-19 hospitalized patients on day t (TOTAL_IN column);
- $E_o(t)$: number of COVID-19 patients entering the hospital (number of lab-confirmed hospital intakes) on day t (NEW_IN column);
- $L_o(t)$: number of COVID-19 patients discharged from the hospital on day t (NEW_OUT column).

The subscript $_o$ stands for “observed”.

We will also mention results obtained with a dataset for France² where t_s is 2020-03-18 and t_e is 2020-07-17.

2.1 Discussion

In the data for Belgium, there is a mismatch between $H_o(t)$ and $H_o(t-1) + E_o(t) - L_o(t)$ for most t and $H_o(t_s) + \sum_{t=t_s+1}^{t_e} E_o(t) - L_o(t)$ is significantly larger than $H_o(t_e)$. This can be due to the patients who get infected at the hospital (they would be counted in H_o without appearing in E_o) and to the patients who die at the hospital (they would be removed from H_o without appearing in L_o). In order to remedy this mismatch, we redefine $L_o(t)$ by $L_o(t) := -H_o(t) + H_o(t-1) + E_o(t)$.

For the French data, we sum the “rad” (daily number of new home returns) and “dc” (daily number of newly deceased persons) columns to get $L_o(t)$. Since there is no column for E_o , we define $E_o(t) = H_o(t) - H_o(t-1) + L_o(t)$.

Several other COVID-19-related data are available. In particular, the daily number of infected individuals, $I_o(t)$, is also reported by health authorities. However, a visual inspection reveals that the graph of I_o is less smooth than the graph of H_o . A possible reason is that I_o is affected by two technical sources of variation: the fraction of tested persons and the accuracy of the tests. In contrast, the reported number of COVID-19 hospitalized individuals, H_o , is expected to be much more accurate. Moreover, for the authorities, predicting H is more crucial than predicting I . Therefore, as in [Koz20], we focus on H .

¹https://epistat.sciensano.be/Data/COVID19BE_HOSP.csv obtained from <https://epistat.wiv-isp.be/covid/>

²[donnees-hospitalieres-covid19-2020-07-17-19h00.csv](https://www.data.gouv.fr/en/datasets/donnees-hospitalieres-covid19-2020-07-17-19h00.csv) obtained from <https://www.data.gouv.fr/en/datasets/donnees-hospitalieres-relatives-a-lepidemie-de-covid-19/>

3 Models

3.1 Case hospitalization ratio

We assume that, for all t ,

$$H(t) = \alpha I(t) \tag{2}$$

where α is unknown but constant over time. In other words, (2) posits that a constant fraction of the infected people is hospitalized.

Equation 2 is reminiscent of [CFP20, (3)], where the number of dead individuals plays the role of H and α is time dependent.

3.2 Observation models

We assume the following observation models with additive noise:

$$H_o(t) = H(t) + \epsilon_H(t) \tag{3a}$$

$$E_o(t) = E(t) + \epsilon_E(t) \tag{3b}$$

$$L_o(t) = L(t) + \epsilon_L(t). \tag{3c}$$

Assuming that the ϵ noises are independent Gaussian centered random variables confers a maximum likelihood interpretation to some subsequent estimators, but this assumption is very simplistic.

3.3 Proposed SH model

Multiplying (1a) and (1b) by α , and multiplying the numerator and denominator of (1a) by α , we obtain

$$\alpha \dot{S}(t) = -\frac{\beta}{N\alpha} \alpha S(t) \alpha I(t) \tag{4}$$

$$\alpha \dot{I}(t) = \frac{\beta}{N\alpha} \alpha S(t) \alpha I(t) - \gamma \alpha I(t). \tag{5}$$

Letting

$$\bar{S} := \alpha S \tag{6}$$

$$\bar{\beta} := \frac{\beta}{N\alpha} \tag{7}$$

and using (2), we obtain the simplified SIR model

$$\dot{\bar{S}}(t) = -\bar{\beta} \bar{S}(t) H(t) \tag{8a}$$

$$\dot{H}(t) = \bar{\beta} \bar{S}(t) H(t) - \gamma H(t) \tag{8b}$$

which we term the *SH model*. (The ‘‘S’’ in this SH model can be interpreted as the number of individuals susceptible of being hospitalized.) The SH model has only two parameters ($\bar{\beta}$ and γ), one hidden state variable (\bar{S}) and one observed state variable (H) with observation model (3a).

Note that, in the SH model (8), the number of patients entering the hospital by unit of time is

$$E(t) := \bar{\beta} \bar{S}(t) H(t) \tag{9}$$

and the number of patients leaving the hospital by unit of time is

$$L(t) := \gamma H(t). \tag{10}$$

4 Estimation and prediction method

The goal is now to leverage the SH model (8) in order to predict future values of H based on its past and current observations $(H_o(t))_{t=t_s, \dots, t_c}$. To this end, we have to estimate (or “learn”) four variables, which we term *estimands*: the two parameters $\bar{\beta}$ and γ and the two initial values $\bar{S}(t_i)$ and $H(t_i)$, where t_i is the chosen initial time for the SH model (8). One possible approach is to minimize some error measure between the simulated values $(H(t))_{t=t_i, \dots, t_c}$ and the observed values $(H_o(t))_{t=t_i, \dots, t_c}$ as a function of the four estimands. However, the error measure is not available as a closed-form expression of the four estimands, and this makes this four-variable optimization problem challenging. We now show that it is possible to estimate $H(t_i)$ and γ separately. This leaves us with an optimization problem in the two remaining estimands $\bar{\beta}$ and $\bar{S}(t_i)$, making it possible to visualize the objective function by means of a contour plot.

4.1 Train and test sets

To recap, we have $t_s \leq t_i < t_c < t_e$. The provided dataset goes from t_s to t_e . The *test set* is $(H_o(t), E_o(t), L_o(t))_{t \in [t_c+1, t_e]}$, and this data cannot be used to estimate the variables and simulate the SH model. The SH model is initialized at t_i , and we refer to the data $(H_o(t), E_o(t), L_o(t))_{t \in [t_i, t_c]}$ as the *train set*, though it is legitimate to widen it to $t \in [t_s, t_c]$.

4.2 Estimation of $H(t_i)$

It is reasonable to believe that ϵ_H in (3a) is small in practice. Hence we simply take

$$H(t_i) := H_o(t_i).$$

4.3 Estimation of γ

We have $L(t) = \gamma H(t)$, see (10). In view of the observation model (3), we can estimate γ by a ratio of means:

$$\hat{\gamma}^{\text{RM}} = \frac{\sum_{t=t_i}^{t_c} L_o(t)}{\sum_{t=t_i}^{t_c} H_o(t)}.$$

Several other estimators are possible, such as the least square estimator, or the total least squares estimator which is the maximum likelihood estimator of γ for the iid Gaussian noise model (3).

Note that t_i in the expression of $\hat{\gamma}$ can legitimately be replaced by any time between t_s and t_c . Only data in the test set, i.e., occurring after t_c , are unavailable in the variable estimation phase.

4.4 Joint estimation of $\bar{\beta}$ and $\bar{S}(t_i)$

We now have to estimate the two remaining estimands, namely $\bar{\beta}$ and $\bar{S}(t_i)$. We choose the following sum-of-squared-errors objective function

$$\phi(\bar{\beta}, \bar{S}(t_i)) = c_H \sum_{t=t_i}^{t_c} (H(t) - H_o(t))^2 + c_E \sum_{t=t_i}^{t_c} (E(t) - E_o(t))^2 + c_L \sum_{t=t_i}^{t_c} (L(t) - L_o(t))^2, \quad (11)$$

where the c coefficients are parameters, all set to 1 in our experiments unless otherwise stated. In (11), $H(t)$, $E(t)$ as in (9), and $L(t)$ as in (10), are given by the (approximate) solution of the SH model (8) in which (i) $H(t_i)$ and γ take the values estimated as above, and (ii) $\bar{\beta}$ and $\bar{S}(t_i)$ take the values specified in the argument of ϕ . In order to compute the required (approximate) solution of the SH model (8), we use the explicit Euler integration with a time step of one day, yielding, for $t = t_i, \dots, t_c - 1$,

$$\bar{S}(t+1) = \bar{S}(t) - \bar{\beta} \bar{S}(t) H(t) \quad (12a)$$

$$H(t+1) = H(t) + \bar{\beta} \bar{S}(t) H(t) - \gamma H(t). \quad (12b)$$

Now that the objective function ϕ (also termed “cost function” or “loss function”) is defined, we let the estimated $(\bar{\beta}, \bar{S}(t_i))$ be the (approximate) minimizer of ϕ returned by some optimization solver.

4.5 Prediction of H

Recall that the time range between t_i and t_c is the train period and the time range between $t_c + 1$ and t_e is termed the test period.

In order to predict the values of H over the test period, we apply the above procedure to estimate the four estimand variables $\bar{\beta}$, γ , $\bar{S}(t_i)$, and $H(t_i)$, and we compute the solution $H(t)$ of (12) for t from t_i to t_e . The prediction is then $(H(t))_{t=t_c+1, \dots, t_e}$. The discrepancy between $(H(t))_{t=t_c+1, \dots, t_e}$ and $(H_o(t))_{t=t_c+1, \dots, t_e}$ reveals the accuracy of the prediction.

5 Alternative estimation and prediction methods

5.1 Successive estimation of $\bar{\beta}$ and $\bar{S}(t_i)$

As an alternative to Section 4.4, we now present a method to estimate $\bar{\beta}$ independently. We do not recommend this alternative, but it sheds light on the various forecast accuracies observed in Section 6.

From (8a) and (9), we obtain

$$\frac{d}{dt} \frac{E(t)}{H(t)} = -\bar{\beta} E(t).$$

Since $\frac{d}{dt} \frac{E}{H} = \frac{H\dot{E} - E\dot{H}}{H^2}$, this yields

$$\bar{\beta} = \frac{\dot{H}(t)}{(H(t))^2} - \frac{\dot{E}(t)}{E(t)H(t)}.$$

Hence a possible estimator for $\bar{\beta}$ is

$$\hat{\bar{\beta}} = \frac{H_o(t+1) - H_o(t)}{(H_o(t))^2} - \frac{E_o(t+1) - E_o(t)}{E_o(t)H_o(t)} \quad (13)$$

and, from (9), a possible simple estimator for the remaining estimand is $\hat{\bar{S}}(t_i) = \frac{E(t_i)}{\hat{\bar{\beta}}H(t_i)}$.

We can now investigate how the ϵ error terms in the observation model (3) impact $\hat{\bar{\beta}}$. We assume throughout that the errors in $H_o(t+1) - H_o(t)$ and $E_o(t+1) - E_o(t)$ are comparable. Except at the very beginning of the outbreak, $E_o(t)H_o(t)$ is considerably smaller than $(H_o(t))^2$, and thus the second term of (13) drives the error.

Consequently, the estimation of $\bar{\beta}$ should be the most accurate when $E_o(t)H_o(t)$ is the largest. This occurs slightly before the peak of $H_o(t)$. This means that the estimation of $\bar{\beta}$ should be the most accurate for a train period slightly before the peak. However, this does not mean that this position of the train period gives the most accurate forecasts, as we will see below.

Let us consider the situation where the train period is located *before* the peak. Then the estimation of $\bar{\beta}$ is less accurate, and this impacts $\hat{\bar{S}}(t_i)$. At the initial time t_i , this does not impact the right-hand term of (8b) in view of the definition of $\hat{\bar{S}}(t_i)$. However, an overestimation of $\bar{\beta}$ will induce an underestimation of $\bar{S}(t_i)$ and, in view of (8a), a subsequent even stronger underestimation of $\bar{S}(t)$. Hence the first term of (8b) will be underestimated. As a consequence, the peak in H will appear sooner and lower. The case of an underestimation of $\bar{\beta}$ leads to the opposite conclusion, namely a peak in H that appears later and higher. In summary, the further before the peak the train period is located, the more inaccurate the position and height of the peak is expected to be.

Finally, let us consider the situation where the train period is located *after* the peak. Then we can make the same observations as in the previous paragraph, except that predicting the peak is now irrelevant. Moreover, we are in the decrease phase, where the first term of (8b) (which involves $\bar{\beta}$ and $\bar{S}(t)$) is smaller than the second term (which does not involve these quantities). Consequently, the possibly large estimation errors on $\bar{\beta}$ and $\bar{S}(t)$ will only slightly affect the forecast of $H(t)$.

5.2 Alternative: joint estimation of the four estimands

An alternative to Sections 4.2–4.4 is to reconsider (11) as a function of all four estimands:

$$\tilde{\phi}(\bar{\beta}, \bar{S}(t_i), \gamma, H(t_i)) = c_H \sum_{t=t_i}^{t_c} (H(t) - H_o(t))^2 + c_E \sum_{t=t_i}^{t_c} (E(t) - E_o(t))^2 + c_L \sum_{t=t_i}^{t_c} (L(t) - L_o(t))^2. \quad (14)$$

In (14), $H(t)$, $E(t)$ as in (9), and $L(t)$ as in (10), are given by the solution of the discrete-time SH model (12) where the parameters $\bar{\beta}$ and γ and the initial conditions $\bar{S}(t_i)$ and $H(t_i)$ take the values specified in the argument of $\tilde{\phi}$. Minimizing $\tilde{\phi}$ is a more challenging problem than minimizing ϕ (11) in view of the larger number of optimization variables. It may be essential to give a good initial guess to the optimization solver, and a natural candidate for this is the values obtained by the procedure described in Sections 4.2–4.4.

In our preliminary experiments, we have found that this alternative does not present a clear advantage in terms of the prediction mean absolute percentage error (MAPE). The results reported in Section 6 are obtained with the sequential prediction approach of Section 4, unless otherwise specified.

6 Results

We now apply the method of Section 4 (by default) or a method of Section 5 (when specified) to the data of Section 2 available for Belgium (by default) and France (when specified).

The methods are implemented in Python 3 and run with Anaconda 2019.10. The code to reproduce the results is available from <https://sites.uclouvain.be/absil/2020.05>.

6.1 Fitting experiment

We first check how well the SH model (8) can fit the available data for Belgium. For this experiment, we use the method of Section 5.2 with $c_E = c_L = 0$ in order to get the best possible fit (in the least squares sense) to the H_o curve. The result is shown in Figure 1.

The fitting error is remarkably small (MAPE below 15%). For the French data, the fit is even better in terms of MAPE (about 3%).

Note that the parameters of the SH model are constant with respect to time in our experiments. This contrasts with [Koz20] where there are two phases, and with [Nes20] where the infection rate is piecewise constant with several pieces.

We stress that Figure 1 tells us little about the prediction capability of the model. If the fit over some period is bad, then predictions (i.e., forecasts) over that period can only be bad. But if the fit is good (as it is the case here), the predictions can still be bad due to their sensitivity with respect to the data preceding the to-be-predicted period. For example, a better fit (in the RMSE sense) than in Figure 1 can be obtained with a polynomial of degree 8; however, its prediction capability is abysmal.

In order to assess the prediction capability of the model, we have to learn the estimand variables over a *train period* that we make available to the algorithm, use the learned estimand variables in order to predict H over a subsequent *test period* (whose data is not available to the algorithm), and finally compare the prediction with the data on the test period. This is what we proceed to do in the rest of this Section 6.

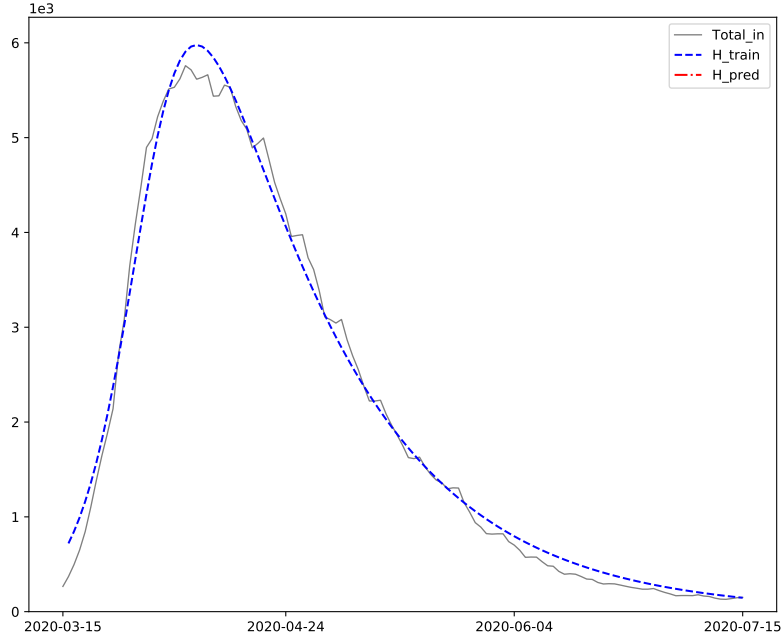


Figure 1: Belgium, fitting the SH model to the H_o (total hospitalized) curve. In this experiment, the train set is the whole dataset, hence there is no test (prediction) curve. Reproduce with SHR_16PA_py_BEL_1sttraintstart1_1sttraintstop123_c100.zip.

6.2 Predictions from a train period around the peak

We start with a prediction experiment where the train period is around the peak. According to Section 5.1, this is a promising location.

A contour plot of the objective function ϕ (11) is given in Figure 2. In order to make the minimizer easier to visualize, the plot shows equispaced-level curves of $\log(\phi - 0.99\phi_*)$, where ϕ_* is an approximation of the minimal value of ϕ . Based on a visual inspection, we choose $(1e-5, 1e4)$ as the initial guess of the optimization solver. The optimization solver is `scipy.optimize.fmin` with its default parameters.

The middle plot of Figure 2 shows $(H_o(t))_{t=t_s, \dots, t_e}$ (observed hospitalizations, gray solid line), $(H(t))_{t=t_i, \dots, t_c}$ (hospitalizations given by the model over the train period, blue dashed line), and $(H(t))_{t=t_c+1, \dots, t_e}$ (hospitalizations predicted over the test period, in red dash-dot line). In order to give a sense of the sensitivity of the results, we superpose the curves obtained for three slightly different train periods. The test MAPE for the three curves are 27%, 7%, and 8%.

The right-hand plot of Figure 2 shows the evolution of $\tilde{S}(t)$.

6.3 Predictions from various train periods

In Figure 3, we superpose the results obtained with various train periods of 14 days. The figure corroborates the comments of Section 5.1.

In particular, if the train period is fully located before the peak, then the predictions are rather inaccurate. Placing the train period around the peak gives excellent prediction results. When the train period is fully located in the decrease phase, the estimation of β and $\tilde{S}(t_i)$ is seen to be very sensitive, but this does not affect much the quality of the prediction of $H(t)$.

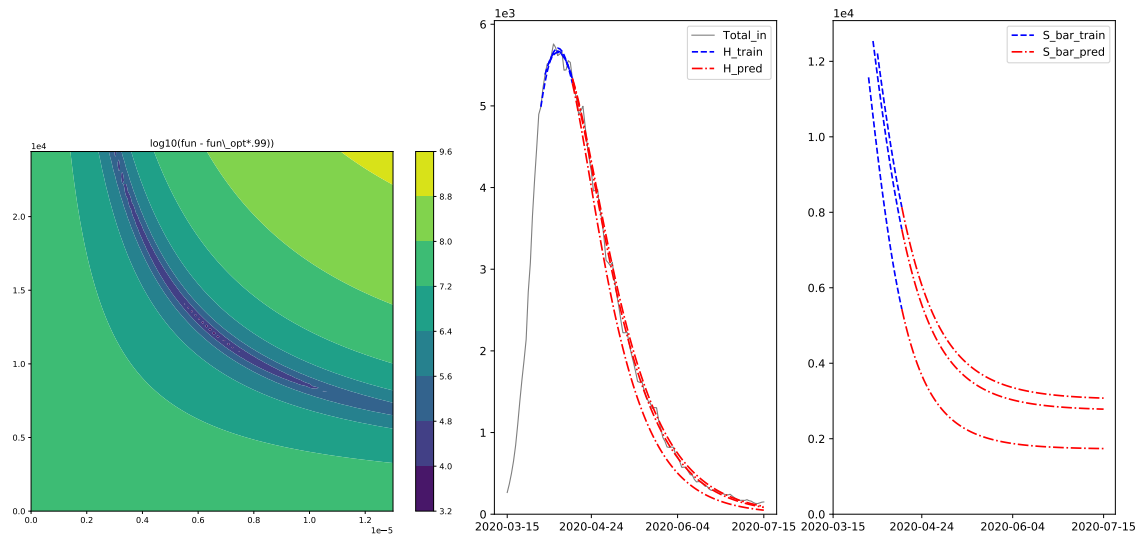


Figure 2: Belgium, train period around the peak. Left: contour plot of ϕ (11). Right: fitting and predictions with the SH model. Reproduce with SHR_16PA_py_BEL_1sttraintstart16_1sttraintstop32_c111.zip.

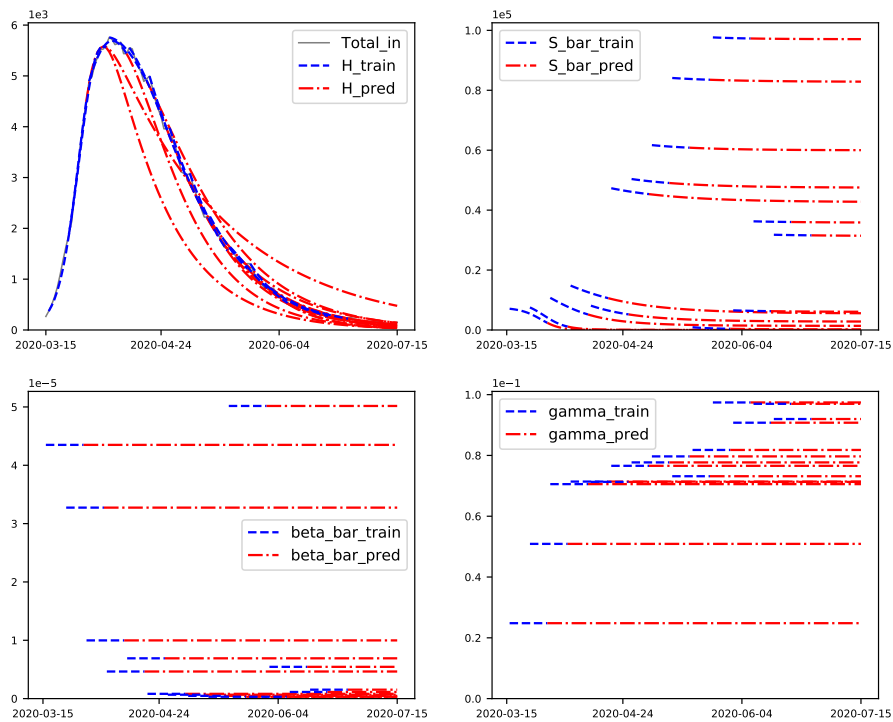


Figure 3: Belgium, various train periods. Reproduce with SHR_16PA_py_BEL_1sttraintstart1_1sttraintstop15_c111.zip.

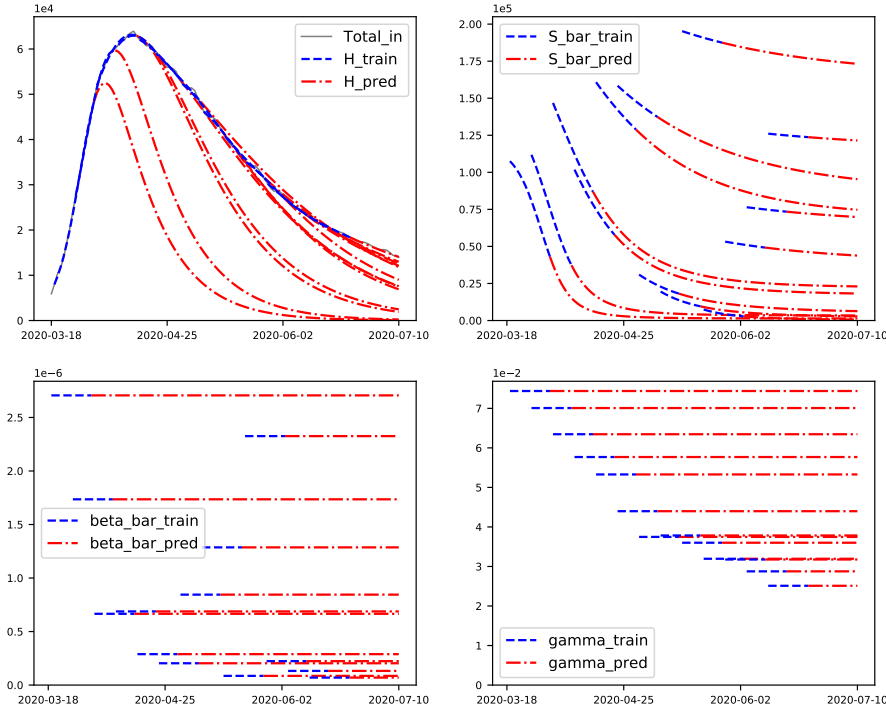


Figure 4: France, various train periods. Reproduce with SHR_16PA_py_FRA_1sttraintstart1_1sttraintstop15_c111.zip.

6.4 Results for France

Figure 4 is the counterpart of Figure 3 for France. These experiments are also compatible with the comments of Section 5.1. We also considered some departments separately, with similar results.

A disconcerting aspect is the evolution of the estimated γ as a function of the location of the train period. In Figure 3 (Belgium), the estimation of γ is grouped around 0.08 for several train periods. However, in Figure 4, the estimation of γ keeps decreasing, indicating that the daily number of patients leaving the hospital is an increasingly small fraction of the number of patients at the hospital.

7 Conclusion

The experiments in Section 6 have shown that the proposed method has a remarkably good fitting capability over the whole available data, and also a remarkably good predictive value over certain time ranges for the Belgian data. However, there are also time ranges where the prediction is very inaccurate, and the accuracy is also found to be lower for the French data. The predictions returned by the model should thus be taken with much caution. In keeping with this warning, we refrained from displaying predictions beyond the end time of the datasets. The Python code is freely available to make such predictions, but there is no warranty on their accuracy.

Another source of caution is that we cannot rule out the situation where the considered objective function would be multimodal. The optimization solver might thus get stuck in a local nonglobal minimum, yielding a suboptimal fit of the train data and possibly a poorer prediction than what an omniscient solver would achieve. Moreover, even if the objective function is unimodal, the stopping criterion of the solver may trigger before an accurate approximation of the minimum is reached.

If the proposed model is used to guide prevention policies, then further caveats are in order.

We have seen that the estimation of $\bar{\beta}$ is very sensitive. Hence the proposed model can hardly help assess the impact of prevention measures on $\bar{\beta}$. Without knowing sufficiently accurately the impact of prevention measures on $\bar{\beta}$, we may not aptly use the model to predict their impact on the evolution of the hospitalizations.

Yet another caveat is that it may be tempting to deduce from the excellent fit with a constant-parameter model (Figure 1) that the evolution of the prevention measures over the dataset period has had no impact on $\bar{\beta}$. But the deduction is flawed. Indeed, in view of the comments made in Section 5.1, the available data could also be very well explained with fairly large jumps in $\bar{\beta}$ during the decrease phase.

In spite of all these caveats, the hospitalization forecasts returned by the method, and also the evolution of $\bar{S}(t)$, might be of practical use in the context of various disease outbreaks, e.g., for resource planning. To this end, it will be important to understand which specific features of the COVID-19 outbreak in Belgium made it possible to forecast so accurately the hospitalization decrease several months ahead.

References

- [Atk20] Andrew Atkeson. What will be the economic impact of COVID-19 in the US? Rough estimates of disease scenarios. Working Paper 26867, National Bureau of Economic Research, March 2020. doi:10.3386/w26867.
- [BD20] Gyan Bhanot and Charles DeLisi. Predictions for europe for the Covid-19 pandemic from a SIR model. *medRxiv*, 2020. doi:10.1101/2020.05.26.20114058.
- [BFG⁺20] Jackie Baek, Vivek F. Farias, Andreea Georgescu, Retsef Levi, Tianyi Peng, Deeksha Sinha, Joshua Wilde, and Andrew Zheng. The limits to learning an SIR process: Granular forecasting for Covid-19, 2020. arXiv:2006.06373.
- [CFP20] Timoteo Carletti, Duccio Fanelli, and Francesco Piazza. Covid-19: The unreasonable effectiveness of simple models. *Chaos, Solitons & Fractals: X*, 5:100034, 2020. doi:10.1016/j.csf.2020.100034.
- [CNP20] Giuseppe C. Calafiore, Carlo Novara, and Corrado Possieri. A modified SIR model for the COVID-19 contagion in Italy, 2020. arXiv:2003.14391.
- [FP20] Duccio Fanelli and Francesco Piazza. Analysis and forecast of COVID-19 spreading in China, Italy and France. *Chaos, Solitons & Fractals*, 134:109761, 2020. doi:10.1016/j.chaos.2020.109761.
- [Het00] Herbert W. Hethcote. The mathematics of infectious diseases. *SIAM Review*, 42(4):599–653, 2000. doi:10.1137/S0036144500371907.
- [KMW27] William Ogilvy Kermack, A. G. McKendrick, and Gilbert Thomas Walker. A contribution to the mathematical theory of epidemics. *Proceedings of the Royal Society of London. Series A, Containing Papers of a Mathematical and Physical Character*, 115(772):700–721, 1927. doi:10.1098/rspa.1927.0118.
- [Koz20] Gregory Kozyreff. Hospitalization dynamics during the first COVID-19 pandemic wave: SIR modelling compared to Belgium, France, Italy, Switzerland and New York City data, 2020. arXiv:2007.01411.
- [LGWR20] Ying Liu, Albert A Gayle, Annelies Wilder-Smith, and Joacim Rocklöv. The reproductive number of COVID-19 is higher compared to SARS coronavirus. *Journal of Travel Medicine*, 27(2), 02 2020. doi:10.1093/jtm/taaa021.

- [Nes20] Yurii Nesterov. Online prediction of COVID19 dynamics. Belgian case study. CORE Discussion Paper 2020/22, UCLouvain, 2020. URL: <https://uclouvain.be/en/research-institutes/lidam/core/core-discussion-papers.html>.
- [RVHL20] Weston C. Roda, Marie B. Varughese, Donglin Han, and Michael Y. Li. Why is it difficult to accurately predict the COVID-19 epidemic? *Infectious Disease Modelling*, 5:271 – 281, 2020. doi:10.1016/j.idm.2020.03.001.
- [SM20] Sudhansu Sekhar Singh and Dinakrushna Mohapatra. Predictive analysis for COVID-19 spread in India by adaptive compartmental model. *medRxiv*, 2020. doi:10.1101/2020.07.08.20148619.
- [WF20] Meimei Wang and Steffen Flessa. Modelling Covid-19 under uncertainty: what can we expect? *The European Journal of Health Economics*, 2020. doi:10.1007/s10198-020-01202-y.